Dentomaxillofacial Radiology (2004) 33, 220–225
© 2004 The British Institute of Radiology
http://dmfr.birjournals.org

RESEARCH

Geometric alignment and chromatic calibration of serial radiographic images

C Dornier*[,1], L Dorsaz-Brossa[1], P Thévenaz[2], F Casagni[3], P Brochut[3], A Mombelli[3] and JP Vallée[1]

[1]Digital Imaging Unit, Division of Medical Computing, Radiology Department, Geneva University Hospital, Switzerland; [2]Biomedical Imaging Group, EPFL, BM-Ecublens, Lausanne, Switzerland; [3]Department of Periodontology, School of Dental Medicine, University of Geneva, Switzerland

Objective: To develop software for automated registration and intensity calibration of serial dental radiographs for the analysis of longitudinal changes in bone density.
Methods: Serial dental radiographs were acquired using a positioning device designed to minimize projection divergence. Each radiograph included an image of a standardized aluminium wedge. The radiographs were scanned on a flatbed scanner (AGFA Duo Scan) with a spatial resolution of 300 dpi, and pixel intensity coded in 16-bit grey scale. The intensity was calibrated using serial images of selected areas with defined thickness of the aluminium wedge. A robust B-splines multiresolution registration algorithm was implemented to overcome the acquisition misalignment. Radiographs, taken before and after periodontal therapy, were subtracted to assess bone density evolution.
Results: The intensity calibration decreased the maximum intensity variations between serial radiographs from 30 ± 17% to 1 ± 1% (mean ± standard deviation), and improved the visual comparison between the radiographs. The registration stage allowed correcting the misalignment of the radiographs on the scanner screen and superimposing the radiography contents. The observed residual motion was about 0.02 ± 0.01 mm.
Conclusion: Very user-friendly software was developed. The manipulator needs to scan the radiographs only one time. The software performs all subsequent processing steps.
Dentomaxillofacial Radiology (2004) **33,** 220–225. doi: 10.1259/dmfr/71716997

Keywords: image registration; bone density; intensity calibration; dental radiographs

Introduction

Periodontal disease leads to changes in the morphology and density of the alveolar bone. To evaluate the success of periodontal therapy, and to determine the stability of an obtained outcome, one would like to quantitatively assess longitudinal changes in the alveolar bone with a simple method. On conventional radiographs, small changes in alveolar bone can hardly be detected since routine radiographs are taken with variation in angulation and without perfectly standardized parameters in exposure and processing. Furthermore, it is known that the human eye can detect changes in sequential radiographs only if they represent an increase or decrease of at least 30–50% in bone mineral content.[1] Invasive or non-invasive methods have been used in the past to assess such changes. Invasive techniques include repeated transgingival probing[2] and direct measurements of the bone morphology during a surgical intervention and at re-entry.[3,4] These methods are limited to the evaluation of the bone profile and are unable to detect density changes. Among the non-invasive techniques, ^{125}I absorptiometry and quantitative radiography have been used in periodontal research.[5] Subtraction of serial radiographs was introduced in the 1930s by Ziedses des Plantes.[6] Small changes in serial radiographs, difficult to visualize by a conventional comparison of images, can be detected using this technique.[7] Photographic methods were used initially for the subtraction of manually aligned *a priori* registered radiographic films. With the emergence of computers, digital subtraction of radiographic images has become possible.[8] Digitized radiographs can be subjected to complex procedures, such as intensity calibration or geometric distortion. Quantitative radiography

*Correspondence to: Christophe Dornier, CO Voirets, Chemin des Voirets 22, Case postale 605, CH-1212 Grand-Lancy 1, Switzerland; E-mail: christophe.dornier@edu.ge.ch
Received 20 August 2003; revised 14 April 2004; accepted 7 May 2004

requires the inclusion of an intensity reference on each radiograph, for example the image of a standardized aluminium wedge, to which bony structures can be related. This reference is also necessary to calibrate the image intensity of serial radiographs.

Correct alignment of serial images is a critical issue for image subtraction.[9] Serial radiographs can be aligned using fixed landmarks, visible on all images, marked for example by three pinholes under an optical microscope. Image registration can be done by using computer.[10,11] This way it becomes possible to realise complex registration algorithms. Two kinds of registration method exist: rigid transformation (only translations and rotation) and non-rigid transformation. In our field, registration based on rigid transformation was sufficient because the serial radiographs were acquired in similar conditions. Some registration processes used prior information and required the identification of some features on each radiograph.[12]

The purpose of this study was to develop software for automated registration and intensity calibration of serial dental radiographs, using an automated registration algorithm based on pixel intensity that does not require prior geometric information (such as pinholes or other landmarks). Analysing serial dental radiographs including a dental implant validated the performance of this algorithm. Calibration and registration steps were validated separately.

Materials and methods

Software was developed using the Interactive Data Language (Interactive Data Language, Research Systems, Inc., CO). Three separate modules were produced, dealing with (i) the digitalization of the radiographs, (ii) the calibration of signal intensity and (iii) the geometric alignment of series of radiographs from the same object.

To evaluate the performance of the newly developed software, standardized dental radiographs were acquired from seven patients (number of available radiographs is reported in Table 1). The radiographs were obtained in the context of a clinical study. The study was approved by the ethical committee of the School of Dental Medicine. All participants gave informed written consent. In order to keep variation of exposure geometry to a minimum, a previously developed paralleling instrument was utilized.[13] Each radiograph included an image of the same aluminium wedge. The radiographs were obtained from an area where a dental implant with precisely known shape and dimensions had been placed.

Digitization of serial dental radiographs

Radiographic images were digitized using a transmission scanner (Duoscan; Agfa-Gevaert N.V., Mortsel, Belgium) with a maximum optical resolution of approximately 2000×1000 dpi (dots per inch). Dental radiographs were scanned with a grey-scale acquisition depth of 16 bits and a spatial resolution of 300 dpi. The radiographs were manually placed over the scan area without any precaution regarding their orientations (large rotations were visible between two images of the same sequence; Figure 1). To ensure an equal size of the scanned images, the radiographs were sequentially processed using the same area for the registration. The scanned radiographs were saved in TIFF format (tagged image file format) supporting 16-bit pixel depth.

Intensity calibration

Repeated images of the same area on the aluminium wedge were used for the calibration of image intensity. A region of interest (ROI) was defined on the aluminium wedge. This ROI was rectangular and was limited to the part of the wedge where its intensity is a strictly monotonic function (Figure 2). To be less sensitive of the overprojection of soft tissues when using the aluminium wedge data for calibration, each intensity profile along the rectangle length was fitted by a third order polynomial (calibration curve). The calibration curves were then modified using a look-up table (LUT) to obtain the same grey values from identical positions on the aluminium wedge on all radiographs (calibration stage). Grey values not represented by the aluminium wedge were transformed to either the maximum or the minimum value of the wedge.

Geometric registration

The purpose of this step is to correct the misalignments of the radiographs' contents after their digitization. Radiographs were processed with IDL software, which acts as front-end to an ANSI-C registration routine.[14] This routine is based on an approach described by Thévenaz and

Table 1 Calibration efficiency assessed by computing dispersion obtained on the mean intensity of the aluminium wedge (global criterion) and by computing mean-square differences per pixel between wedge profiles (local criterion)

		Global criterion		*Local criterion*	
	Number of available radiographs	*Scanned images (%)*	*Calibrated images (%)*	*Scanned images*	*Calibrated images*
Patient 1	2	25.77	0.16	0.1245	0.0393
Patient 2	2	30.89	1.77	0.1152	0.0341
Patient 3	2	56.74	0.94	0.2012	0.0541
Patient 4	3	18.86	0.07	0.0852	0.0422
Patient 5	3	15.11	2.81	0.0875	0.0582
Patient 6	5	47.78	0.93	0.1807	0.0334
Patient 7	5	14.14	0.38	0.0774	0.0630
Mean		29.90	1.01	0.1245	0.0463
Standard deviation		16.57	0.98	0.0488	0.0120
Value of the *t*-test		$P < 0.004$		$P < 0.008$	

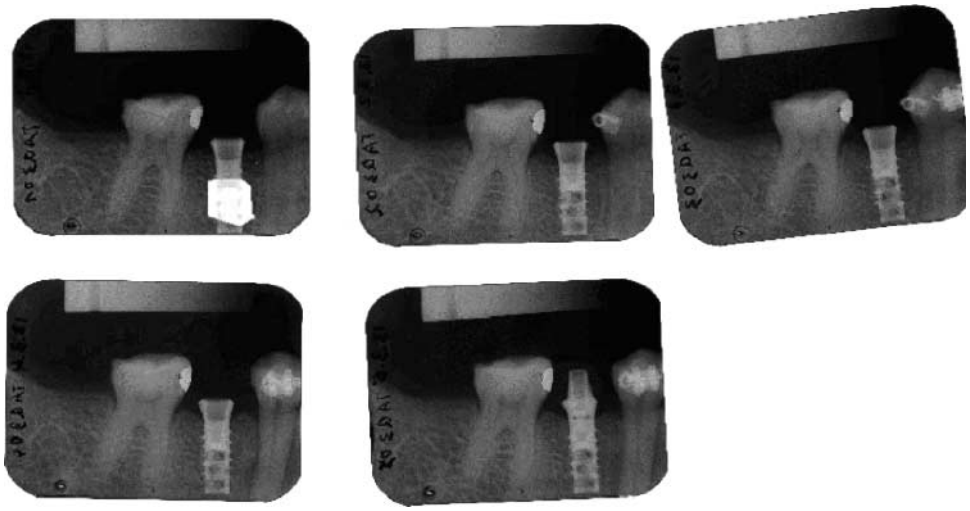

Figure 1 Example of scanned serial dental radiographs. The region of interest (ROI) (in video inverse) on the first frame represents the area used for performing the geometric registration. The ROI is always placed over the implant location

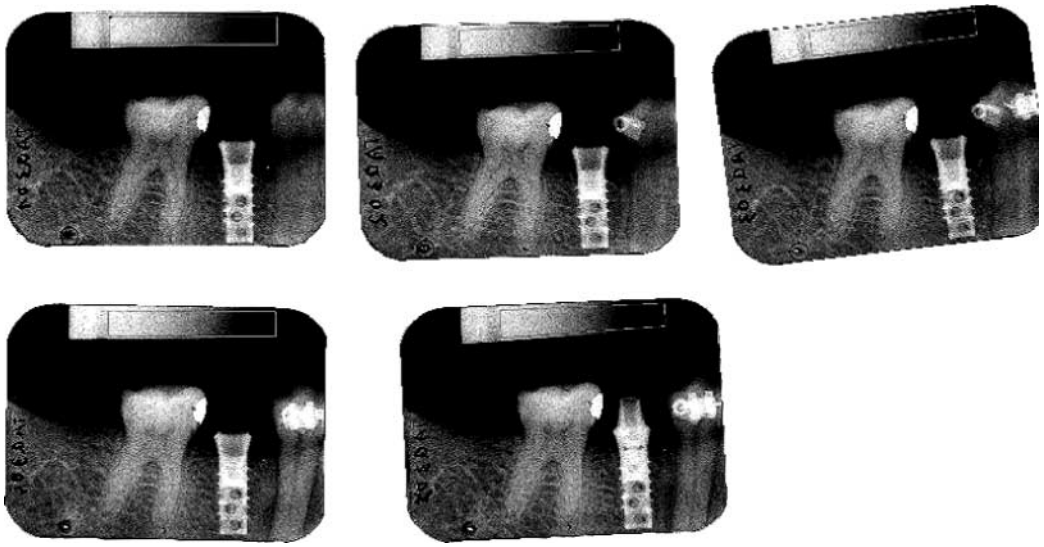

Figure 2 Definition of the region of interest (ROI) for performing the intensity calibration. A polygonal ROI was drawn over the aluminium wedge on each digital radiograph. Calibration curves are obtained by fitting the intensity profile along the rectangle length by a third order polynomial

Unser.[15] The algorithm works directly on pixels intensity. One image was defined as the target image and this image was the reference for the registration process. All other images (test images) were sequentially registered to the target image. The registration process aims at a minimization of the grey-scale differences between two images (the target image and one of the test images). To achieve sub-pixel efficiency in the registration process, geometric operations were not realised directly on the sampled images but on a continuous model (based on B-splines of degree n).[16,17] The registration was performed in a multiresolution scheme to decrease the computation time. The registration process can be limited to a part of the image by drawing ROIs.

The geometric registration stage is realised in practice by drawing one ROI, centred on the area to be registered (implant), in one frame (Figure 1). The registration algorithm will then translate and rotate all other images of the same sequence in order to obtain the image of the implant at the same position over all the other images.

Validation of the intensity calibration

The intensity calibration was validated by two methods. The first method used a global approach that consisted of calculating, for each patient, the mean intensity inside the aluminium wedge over all radiographs. The global criterion was obtained by dividing the maximum dispersion by the average of these mean intensities (see Equation 1).

$$\frac{\text{Max.}(\{\bar{I}\}) - \text{Min.}(\{\bar{I}\})}{\text{Average}(\{\bar{I}\})} \qquad (1)$$

where $\{\bar{I}\}$ represents the set of the mean intensities of the wedge for each patient.

The second method was based on a local approach and consisted of computing the mean-square differences (MSD) per pixel between each intensity profile and the mean intensity profile (see Equation 2).

$$\frac{\sum_{x=1}^{n} \frac{\sum_{i=1}^{nb} [I_i(x) - \bar{I}(x)]^2}{nb}}{n} \quad (2)$$

where n represents the length of the wedge, nb is the number of radiographs in the patient's study, I represents the intensity along the wedge length, and $\bar{I}$ represents the intensity mean along the wedge length for the nb radiographs.

Validation of the geometric registration
The geometric registration stage was validated by computing the residual motion and misalignments observed between the different serial dental radiographs. This was realised by moving a ROI with the implant shape over each image. This ROI with an implant shape was manually translated and rotated until the ROI overlapped exactly the implant on each radiograph. The control was visually realised and the position of the ROI and its orientation were calculated in each radiograph.

The radiographs used in this study had already been registered under an optical microscope for a previous analysis. Three marks had been made manually, identifying the positioning of repeated images. In order to compare the manual registration process under an optical microscope with this automatic registration stage, the standard deviation of the displacements of these marks between repeated radiographs was assessed after registering the images with our method.

Results

Intensity calibration
The method derived from the global criterion shows clearly the efficiency of the calibrating stage (Table 1). Measurements performed directly on scanned radiographs obtained from seven patients led to a dispersion of 29.90 ± 16.57% (mean ± standard deviation) in mean intensity in repeated scans of the wedge. The calibrating stage was able to reduce this variability of image intensity to 1.01 ± 0.98. This improvement was statistically significant (*t*-test, $P < 0.004$).

With the method using a local approach, the calibration step decreased the average MSD by a factor of 2 and reduced its standard deviation over four times. This improvement was also statistically significant (*t*-test, $P < 0.008$).

Geometric registration
Table 2 illustrates the variation in positioning of the implant on the radiographs when measurements were performed on scanned images directly ("No registration") and on the images where the registration was performed on the implant ("Registration of radiographic content"). For both translation and rotation parameters, the improvement due to the geometric registration stage was also statistically significant (*t*-test, $P < 0.016$ for *X*-translation; $P < 7 \times 10^{-5}$ for *Y*-translation; and $P < 4 \times 10^{-4}$ for the angle parameter).

Figure 3 presents the registration process in a more visual manner. For one patient we observed that the subtraction of all subsequent radiographs from the first radiograph did not cancel the image of the implant when using the scanned images directly. When the subtraction operation was performed on the images after geometric correction, the implant became invisible over all frames, indicating that its position did not change along the registered images.

The discrepancy between manual (three marks placed manually) and this automatic registration amounted to 2.1 pixels in mean and 1.6 pixels in dispersion (pixels are 0.08 mm wide).

Discussion

This study shows that accurate intensity calibration and image registration can be achieved with very user-friendly software, allowing persons without an expertise in computer technology to study bone density evolution over time easily. The processing time of serial dental radiographs can be decreased significantly by using our digital registration process instead of a conventional optical registration process.

One goal of this study was to measure the positional variation of the implant on the dental serial radiographs after geometric registration. A pixel depth of 16 bits and a spatial resolution of approximately 300 dpi were chosen for digitizing dental radiographs. This resolution yielded a pixel size of approximately 0.08 mm, which was sufficient for assessing the position of the implant on the image. The size of the radiographs was equal to 480 × 363 pixels and a dental implant was depicted by more than 6500 pixels.

On a Pentium III computer (733 MHz) with 512 Mo RAM and with a non-optimized coding, the computation time t_{cal} for performing the calibration stage was 0.46 s per image. The computational time t_{reg} for the geometric registration stage was 4.8 s. For both steps the computation time is linearly correlated to the number of pixels on the images (Table 3). The computation time for each stage can be expressed as a function of the number of pixels *npix*, as follow:

$$t_{cal} = 9 \times 10^{-6}\, npix + 0.22$$

$$t_{reg} = 8 \times 10^{-5}\, npix + 7.91$$

These computation times do not include the scanning stage, which is the most time consuming procedure. The scanning stage is necessary for the analysis of dental radiographs acquired with the classical analogue X-ray method. It would not be necessary if a digital acquisition method were used.

Table 2 Registration efficiency: comparisons of the positional variations of the dental implant

	Translation (pixels)					
	X		*Y*		*Angle (degrees)*	
Registration technique	*min. mean*	*max. SD*	*min. mean*	*max. SD*	*min. mean*	*max. SD*
No registration	1.4	14.4	0.0	13.5	0.0	7.9
	5.9	4.5	6.4	4.0	3.2	2.5
Registration of radiographic content	0.0	0.7	0.0	0.8	0.0	1e − 6
	0.3	0.3	0.2	0.3	2e − 7	5e − 7
Value of the *t*-test	$P < 0.016$		$P < 7 \times 10^{-5}$		$P < 4 \times 10^{-4}$	

Pixels are 0.08 mm wide; SD, standard deviation

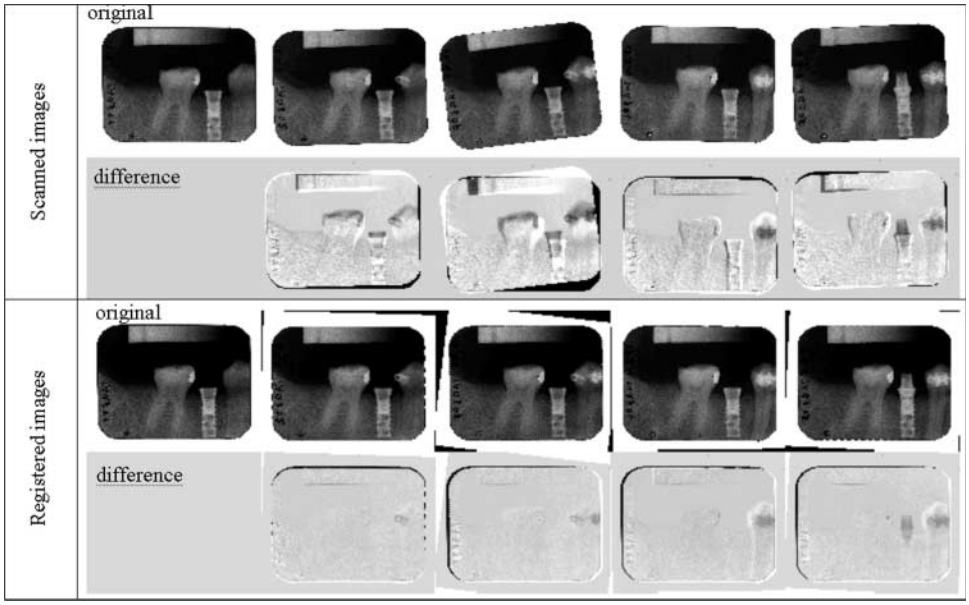

Figure 3 Example of serial dental radiographs before and after the registration process performed on the implant area. The first two lines present the scanned radiographs and the difference between each radiograph to the first radiograph. The last two lines present the same images after performing the registration stage. On difference images, the implant is clearly visible on scanned images owing to misalignment and it becomes invisible after the registration process

In the validation of the intensity calibration stage, the first criterion emphasises the fact that the calibration stage is well suited for obtaining serial dental radiographs with the same distribution of the grey values inside the aluminium wedge. The second criterion shows that the range of the grey values inside the aluminium wedge between serial dental radiographs is more accurate after the calibration stage.

Comparing the manual and automatic registration process, the observed discrepancy emphasises the limitation of manual alignment of serial radiographs. Figure 4 shows the largest differences obtained in the position of one mark. Using the registration method presented in this paper leads to better results than those obtained with a manual registration including the perforation of each radiograph at three points.

Table 3 Computation time per image for different spatial resolutions

	Spatial resolution		
	300 dpi	*500 dpi*	*800 dpi*
Pixels number	247050	686250	1756535
Calibration time (s)	0.46	1.22	3.03
Registration time (s)	4.801	14.02	30.06

The algorithm used in this study for performing the geometric registration was limited to two-dimensional (2D) rigid body. For the acquisition of the serial dental radiographs a mechanical aiming device was placed in the mouth.[18] This device limits incongruity in projection of repeated radiographs. The angular variation was below a 1.4° threshold in 91% of all series of repeated radiographs in a study using this method.[19] Since radiographs provide a planar projection of a 3D object crossed by X-rays, the geometric registration stage can correct translations and rotations in the radiography plane. With the use of a mechanical device, the distance between teeth and radiographic film remains constant, thus it was not necessary to implement a scale correction in the registration stage. Residual angular misalignment between radiographs cannot be corrected because radiographs are planar projections of the imaging area and all volume information is flattened.

As this registration algorithm is able to perform 3D registration, the software can be easily updated to process

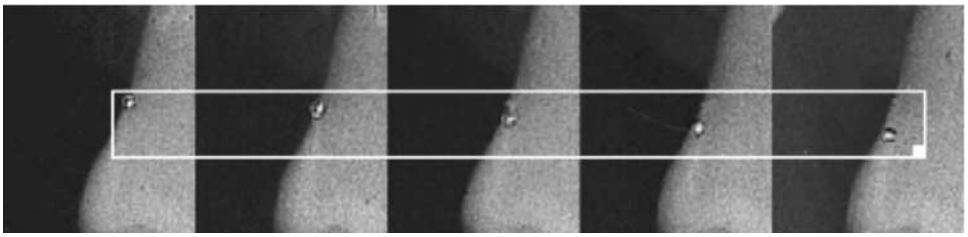

Figure 4 Serial images of the same mark performed under an optical microscope on a molar tooth. The five images were registered with the automatic algorithm. The misalignment of the mark between the different radiographs was easily observed. This example corresponded to the worst case included in this study

3D data sets obtained from tuned aperture computed tomography (TACT™).[20,21] This acquisition modality performs several 2D acquisitions with different orientations and the 3D volume is reconstructed from all the 2D images.

Subtraction radiography provides obvious advantages in image analysis and allows the detection of changes that cannot be seen by simple comparison of sequential radiographs. Nevertheless, this technique has not become part of the dental diagnostic routine, mainly because the efforts necessary for standardization and alignment have been very high so far. The techniques presented in this paper significantly simplify and improve these procedures. With the advent of digital image acquisition, the use of digital image enhancement is further simplified because the scanning of the images is no longer necessary. These developments will further enhance the diagnostic usefulness of radiographic diagnosis in dentistry, particularly for the monitoring of small tissue changes over time.

Acknowledgment
The authors thank Christian Girard for help in the digitization of the dental radiographs.

References

1. Jeffcoat MK, Wang IC, Reddy MS. Radiographic diagnosis in periodontics. *Periodontol 2000* 1995; **7:** 54–68.
2. Durwin A, Chamberlain H, Garrett S, Renvert S, Egelberg J. Healing after treatment of periodontal intraosseous defects. IV Effect of a non-resective versus a partially resective approach. *J Clin Periodontol* 1985; **12:** 525–539.
3. Polson AM, Heijl LC. Osseous repair in infrabony periodontal defects. *J Clin Periodontol* 1978; **5:** 13–23.
4. Froum SJ, Coran M, Thaller B, Kushner L, Scopp IW, Stahl SS. Periodontal healing following open debridement flap procedures. I. Clinical assessment of soft tissue and osseous repair. *J Periodontol* 1982; **53:** 8–14.
5. Haussmann E. A contemporary perspective on techniques for the clinical assessment of alveolar bone. *J Periodontol* 1990; **61:** 149–156.
6. Lehmann TM, Gröndahl HG, Benn DK. Computer-based registration for digital subtraction in dental radiology. *Dentomaxillofac Radiol* 2000; **29:** 323–346.
7. Brägger U, Pasquali L, Rylander H, Carnes D, Kornman KS. Computer-assisted densitometric image analysis in periodontal radiography. *J Clin Periodontol* 1988; **15:** 27–37.
8. Lee SH, Kim EK. Development of subtraction radiography system by using personal computer. Proceedings of the 10th International Congress of Dento-Maxillo-Facial Radiology; 1994, pp 371–376.
9. Benn DK. Limitations of the digital image subtraction technique in assessing alveolar bone crest changes due to misalignment errors during image capture. *Dentomaxillofac Radiol* 1990; **19:** 97–104.
10. Lehmann T, Sovakar A, Schmitt W, Repges R. A comparison of similarity measures for digital subtraction radiography. *Comput Biol Med* 1997; **27:** 151–167.
11. Lehmann TM, Gröndahl HG, Benn DK. Computer-based registration for digital subtraction in dental radiology. *Dentomaxillofac Radiol* 2000; **29:** 323–346. Erratum in: *Dentomaxillofac Radiol* 2001; **30**: 64.
12. Ettinger GJ, Gordon GG, Goodson JM, Socransky SS, William R. Development of automated registration algorithms for subtraction radiography. *J Clin Periodontol* 1994; **21:** 540–543.
13. Graf JM, Mounir A, Payot P, Cimasoni G. A simple paralleling instrument for superimposing radiographs of the molar regions. *Oral Surg Oral Med Oral Pathol* 1988; **66:** 502–506.
14. Thévenaz, P. Intramodal registration software. E-mail: http://bigwww.epfl.ch/thevenaz/registration/
15. Thévenaz P, Unser M. A pyramid approach to subpixel registration based on intensity. *IEEE Trans Image Process* 1998; **7:** 27–41.
16. Unser M. Splines: a perfect fit for signal and image processing. *IEEE Signal Proc Mag* 1999; **16:** 22–38.
17. Thévenaz P, Blu T, Unser M. Interpolation revisited. *IEEE Trans Med Imaging* 2000; **19:** 739–758.
18. Dubrez B, Graf JM, Vuagnat P, Cimasoni G. Increase of interproximal bone density after subgingival instrumentation: a quantitative radiographical study. *J Periodontol* 1990; **61:** 725–731.
19. Dubrez B, Jacot-Descombes S, Cimasoni G. Reliability of a paralleling instrument for dental radiographs. *Oral Surg Oral Med Oral Pathol Oral Radiol Endod* 1995; **80:** 358–364.
20. Webber RL, Horton RA, Underhill TE, Ludlow JB, Tyndall DA. Comparison of film, direct digital, and tuned-aperture computed tomography images to identify the location of crestal defects around endosseous titanium implants. *Oral Surg Oral Med Oral Pathol Oral Radiol Endod* 1996; **81:** 480–490.
21. Webber RL, Horton RA, Tyndall DA, Ludlow JB. Tuned-aperture computed tomography (TACT). Theory and application for three-dimensional dento-alveolar imaging. *Dentomaxillofac Radiol* 1997; **26:** 53–62.